

Supporting Information

**Amino-modified zirconia aerogels for the efficient filtration
of NO₂: Effects of water on the removal mechanisms**

Xinbo Wang, Kai Li, Guojie Liang, Yue Zhao, Ruyue Su, Zhiqiang Luan, Li Li*,
Hailing Xi*

State Key Laboratory of NBC Protection for Civilian, Research Institute of Chemical
Defense, Beijing 100191, China

*Corresponding author. E-mail: lily97@buaa.edu.cn xihailing@sklnbcpc.cn

Number of Tables: 6; Number of Figures: 7.

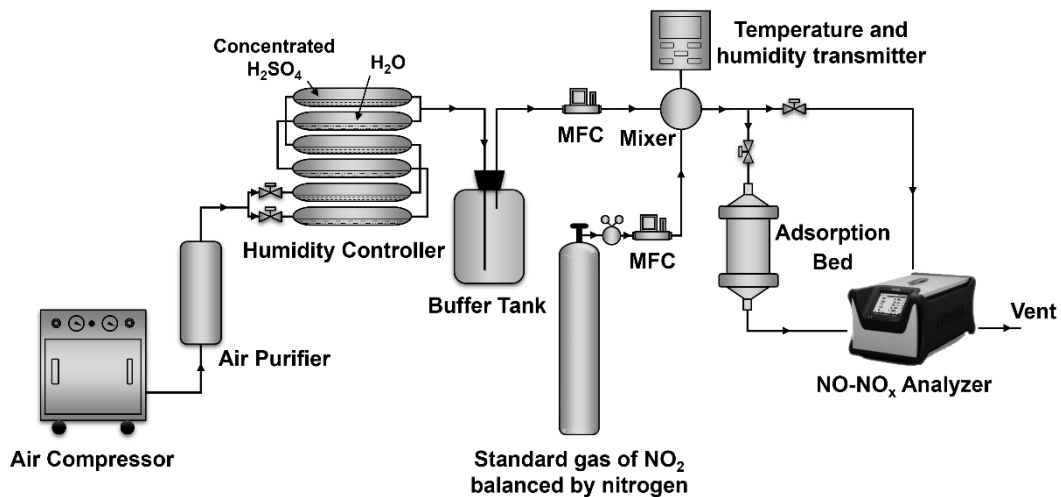


Figure S1. Tube breakthrough system for granule samples.

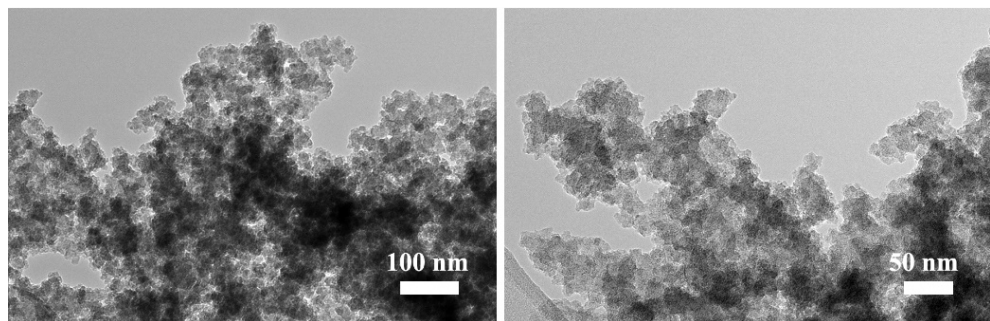


Figure S2. TEM images for AMZA-4.

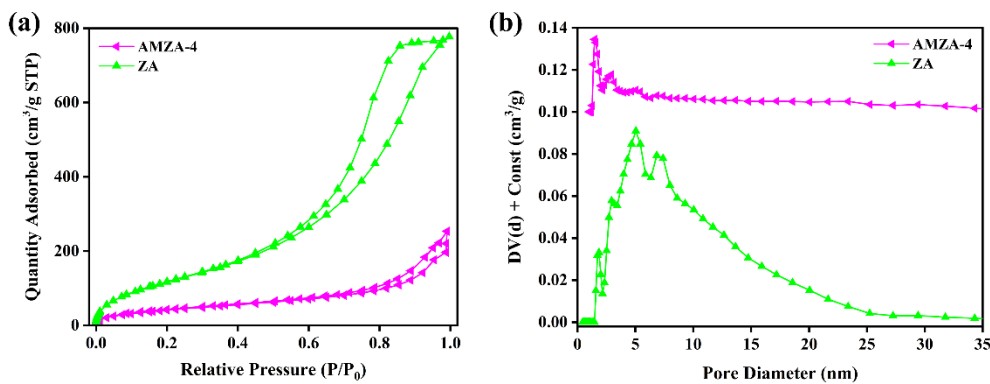


Figure S3. (a) Ar adsorption-desorption isotherms at 87 K and (b) NLDFT pore size distribution of the ZA and AMZA-4 aerogel samples.

Table S1. Texture properties of the ZA and AMZA-4 aerogel samples derived from Ar porosimetry at 87 K

Sample	$V_{\text{micro}}/(\text{cm}^3 \cdot \text{g}^{-1})$	$V_{\text{total}}/(\text{cm}^3 \cdot \text{g}^{-1})$	$\frac{V_{\text{micro}}}{V_{\text{total}}} / \%$
ZA	0.02	0.97	2
AMZA-4	0.02	0.58	3

Table S2. Comparison of the bulk density for ZA and AZMA-4 aerogels

Sample	Density ($\text{cm}^3 \cdot \text{g}^{-1}$)
ZA	0.39
AMZA-4	0.45

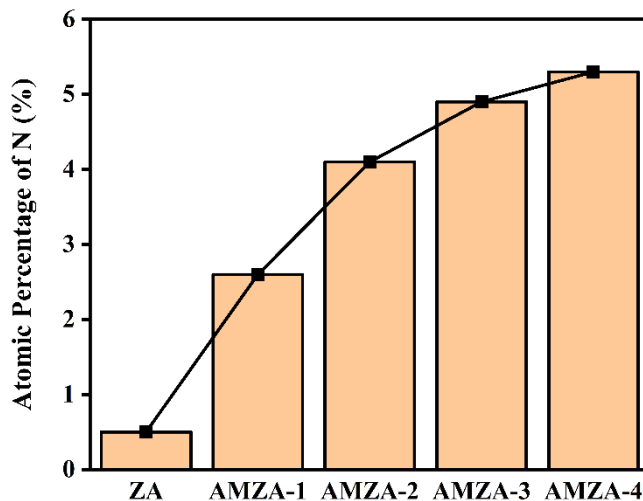


Figure S4. Atomic percentage of the surface N element derived from XPS survey scans for samples obtained with different APTES amount.

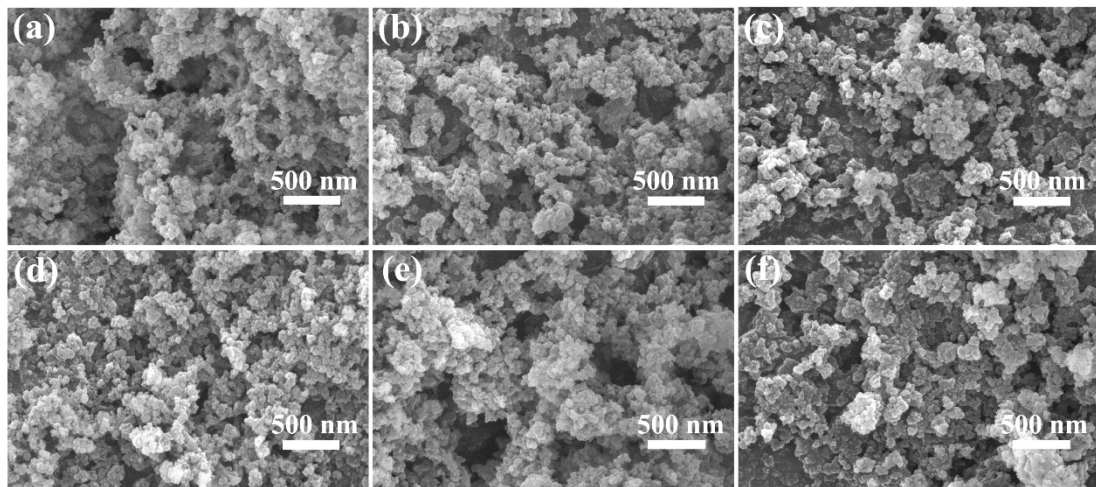


Figure S5. SEM images of (a) fresh AMZA-4 sample and those exposed to NO₂ under different humidity conditions: (b) RH 0-15%, (c) RH 0-50%, (d) RH 50-50%, (e) RH 80-80%, and (f) RH 0-80%.

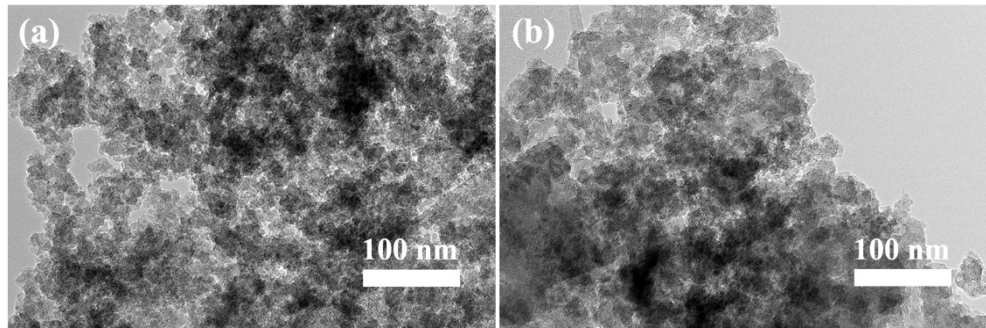


Figure S6. TEM images of the AMZA-4 sample (a) prior to and (b) following NO₂ adsorption at RH 0-80%.

Table S3. Comparison of texture properties of the AMZA-4 samples derived from N₂ porosimetry at 77 K before and after NO₂ adsorption

Sample/ RH	Breakthrough time/min	$S_{\text{BET}}/(\text{m}^2 \cdot \text{g}^{-1})$	$V_{\text{meso}}/(\text{cm}^3 \cdot \text{g}^{-1})$	$V_{\text{total}}/(\text{cm}^3 \cdot \text{g}^{-1})$	$\frac{V_{\text{meso}}}{V_{\text{total}}}\%$	D_{avg}/nm
AMZA-4	—	197.0	0.65	0.67	97	27.8
0-15%	130	175.8	0.60	0.62	97	31.3

0-50%	197	151.3	0.54	0.56	96	30.9
50-50%	205	156.5	0.50	0.51	98	32.5
80-80%	220	127.4	0.45	0.46	98	34.3
0-80%	362	103.8	0.39	0.40	98	39.2

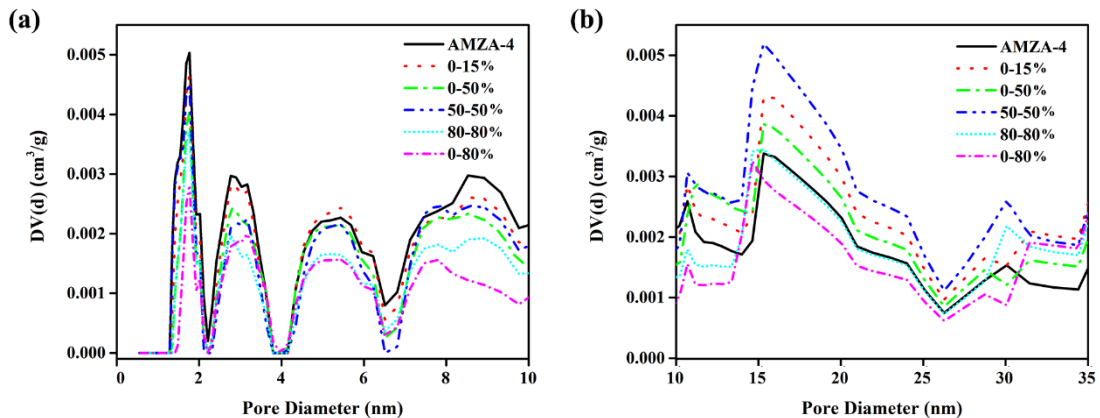


Figure S7. Alterations in the DFT pore size distributions of AMZA-4 samples after NO_2 adsorption under different humidity conditions: (a) the pore $< 10 \text{ nm}$, (b) the pore in the range of $10\text{--}35 \text{ nm}$. Data were derived from N_2 porosimetry at 77 K .

Table S4. The surface elemental composition and atomic percentage of AMZA-4 before and after NO_2 adsorption

Sample/RH	Atomic percentage/%					$\Delta\text{O}/\Delta\text{N}$
	C	N	O	Zr	Si	
AMZA-4	29.7	5.3	44.5	1.3	19.2	—
0-15%	29.2	5.8	45.1	1.2	18.7	1.2
0-80%	27.0	6.7	46.4	1.3	18.6	1.4
80-80%	27.1	6.2	46.9	1.4	18.4	2.7

Table S5. Ratios of different NO_2 adsorption products and percentages of protonated amino groups under different humidity conditions

Sample/RH	Nitrates/ (nitroamines + nitrosamines)	Percentages of protonated amino groups $-\text{NH}_3^+/-\text{NH}_3^+ + -\text{NH}_2$
AMZA-4	—	0.26

0-15%	0.40	0.31
0-80%	1.97	0.36
80-80%	1.07	0.43

Table S6. Existing patterns and relative atomic percentage of the N element on the AMZA-4 surface before and after NO₂ exposure

Sample/RH	Species	FWHM/eV	Peak position/eV	Peak area	Fraction/%
AMZA-4	-NH ₂	2.0	399.4	21696.6	73.7
	-NH ₃ ⁺	2.0	401.2	7738.9	26.3
0-15%	-NH ₂	1.9	399.6	19472.1	52.9
	-NH ₃ ⁺	1.8	401.1	8817.4	23.9
0-80%	Nitrosamine	1.4	402.2	3238.4	8.8
	Nitramine	1.3	406.5	2884.6	7.8
	Nitrate	1.6	407.0	2422.5	6.6
80-80%	-NH ₂	2.0	399.8	14092.5	45.2
	-NH ₃ ⁺	1.8	401.6	8017.9	25.7
	Nitrosamine	1.3	402.5	1551.1	4.97
80-80%	Nitramine	1.1	406.3	1506.9	4.83
	Nitrate	1.4	407.0	6033.9	19.3
	-NH ₂	1.9	399.7	11733.0	40.6
80-80%	-NH ₃ ⁺	1.9	401.4	8599.2	29.7
	Nitrosamine	1.4	402.3	2355.6	8.2
	Nitramine	1.1	406.4	1769.4	6.1
80-80%	Nitrate	1.4	407.0	4453.5	15.4